FLOW FEATURES IN A RENEWED WIND TUNNEL

A. Piccato, P.G. Spazzini and R. Malvano
Istituto Nazionale di Ricerca Metrologica (INRIM)
Strada delle cacce, 91 ï 10135 Torino, Italy
Contact Author: P.G. Spazzini ï p.spazzini@inrim.it

Abstract

In the present paper, the preliminary tests conducted about a renewed wind tunnel are described. The test rig was deeply reviewed during these last two years. The works were performed focussing on the aim of improving the metrological features of the device in view of its use within the definition of an airspeed standard.
Measurements of maximum airspeed and flow fluctuation along the test chamber axis are presented here.

1- Introduction

Wind tunnels find application in several fields of modern technology, from aerospace/automotive testing to validation of wind energy generators. Their aim is to produce a stream of air in controllable and reproducible conditions, and to this aim they are provided with various instruments allowing to measure the velocity of the air stream, its features, and the associated uncertainty.
In the field of metrology, one important use of wind tunnels is the calibration of anemometers. Such instruments are aimed at the measurement of the air speed and they find their application in the aerospace field (monitoring of wind conditions in airports, airplanes airspeed), energy and environment (wind monitoring for wind farms/chimneys), meteorology, ventilation, etc. There exists a wide variety of anemometer types, ranging from the mechanical to the thermal, ultrasonic, laser Doppler and so on.
Two wind tunnels are available at INRIM for the calibration of anemometers. The present paper deals with the characterization of one of them and the establishment of its metrological features.

2- The GVP Tunnel

The wind tunnel discussed in the present paper is the smaller of those available to INRIM for anemometer calibration; it is known as GVP, for Galleria del Vento Piccola (Small Wind Tunnel). It is an open-circuit, semi-open test chamber tunnel, with engine and fan downstream of the test chamber. A picture of the tunnel in its present state is reported in Fig. 1.
Its original construction dates back to the õ30s of last century, and it was upgraded several times since. A few years ago, it was decided to proceed to a further renovation aimed at improving the metrological features of the test rig. Specifically, since the previous renovation (which focused on lower speeds) a vibration of the tunnel at high speed was observed, which somewhat disturbed the measurements. Also, the flow conditions in the divergent were not optimal, the fan was of low quality and the structure supporting the test chamber had a limited rigidity.
The renewed design faced all these limitations: the divergent and the fan were redesigned based on the original ones, which had an excellent flow quality but unfortunately were built in wood and were therefore no more usable due to the decay of the material. The new parts are now built in metal alloys and are expected to have a good duration. A very rigid structure for the test

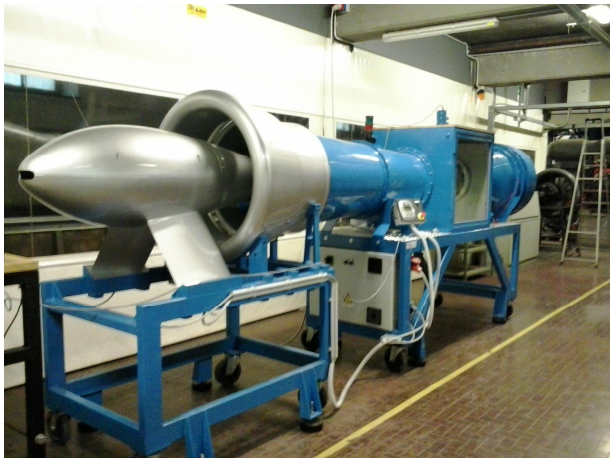

Fig. 1. Picture of GVP in its present condition.

chamber support was designed; the door frames were also improved.
A full account of the redesign of the facility, together with all the preliminary evaluations performed in this work, can be found in [1].
Prior to the renovation works, a full mapping of the flow in the test chamber was performed for comparison purposes. Detailed results of this mapping are reported and commented in [2]. In general, it was observed that the test rig could provide a generally acceptable flow quality, but several small drawbacks were present and could be corrected to improve the metrological features of the standard.

3- Measurement Instruments

The monitoring of the airspeed in the GVP test chamber is obtained by means of two static pressure rings positioned at the entrance and at the exit sections of the convergent. The pressure drop across the convergent is

put in relation with the airspeed at the measurement point, which is located on the axis of the tunnel, 10 cm downstream of the convergent exit section.
The airspeed at the measurement point during wind tunnel calibration is measured by means of an LDA traceable to the Italian national standards of length and time. In order to perform the calibration using comparable quantities, the actual velocity at the measurement point measured by the LDA is plotted against the pseudo-velocity computed by the Bernoulli law using the pressure drop across the convergent and the current ambient thermodynamic conditions. Fig. 2 reports the graph of the wind tunnel calibration thus obtained.

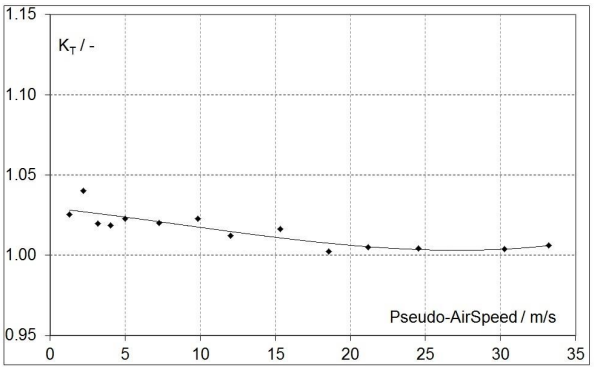

Fig. 2. GVP calibration: relationship between pseudo-velocity computed from convergent conditions and LDA readings..

The calibration data are expressed in terms of a coefficient of calibration of the tunnel as a function of the pseudo-speed based on the pressure drop across the convergent. It can be observed that the resulting coefficient of calibration has a flat behaviour, indicating a good regularity of functioning of the test rig. The value is close to 1, and displays a slight decrease with increasing velocity.
For the analysis of the flow quality, a Hot Wire anemometer was used; the HW was placed at several positions along the test chamber axis, namely at X_1 = 10 cm, X_2 = 20 cm, X_3 = 30 cm and X_4 = 40 cm downstream of the convergent exit; measurements were performed at several wind tunnel speeds. The aim of these tests was to determine the level of fluctuation of the flow at these positions for different flow regimes. Fig. 3 shows a picture of the hot wire sensor mounted in the wind tunnel test chamber (pos. X_1).
A one-component DANTEC 9055P0111 straight probe was used for the measurements; the probe was connected to a DANTEC 55M10 high-precision anemometric bridge which generated a voltage signal, subsequently read by a NI 16-bit DAQ board equipped with a sample-and-hold module. Data were recorded by means of a dedicated software written in LabVIEW™ 6.1.

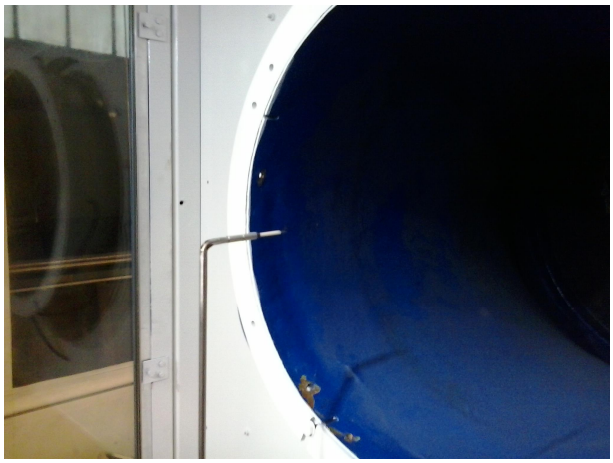

Fig. 3. Hot Wire sensor in the GVP test chamber.

Hot wire electrical signals were converted to velocity using a dedicated software.
First of all, the hot wire was calibrated in situ using the wind tunnel itself as a calibration rig. Fig. 4 shows the graph of the linearized calibration data:

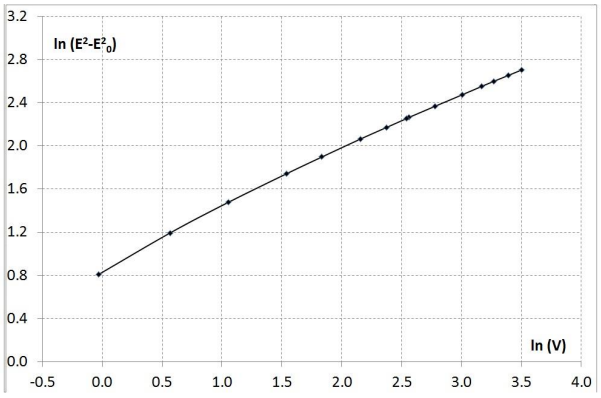

Fig. 4. HW calibration: linearized relationship between velocity and voltage.

The velocity signals were afterwards analysed to obtain average velocities, turbulence intensities and, in particular, spectral energy densities.
The latter analysis was performed by Fourier decomposition of the signals.
The Fourier decomposition technique applied here is based on a standard FFT algorithm (see, e.g. [5]), with breaking up of the signal in subsignals to improve the stability of the result; Hanning windowing is also applied to the subsignals, which were set in such a way to enable the measurement of frequencies as low as 0.1 Hz.

4- Results.

4.1 Test chamber airspeed:

The first measurements that were performed were related to the airspeed value in the test chamber.
With the previous configuration, the GVP was able to cover a range included between 0.5 and 25 m/s,

although the tunnel was qualified and certified for the range 2 m/s ÒV Ò25 m/s. This limitation was due to the fact that the reference airspeed was measured by means of the pressure drop across the convergent and calibrated against a static-Pitot tube in the measurement position. The measurement was therefore traceable to the national standard of pressure. Due to the high uncertainties connected to the measurement of low airspeeds with pressure-based methods, it had been established to limit the minimum speed to the aforementioned value.
In its present state, on the other hand, the traceability is to the national standards of length and time through an LDA. Indeed, although the ordinary working condition of the tunnel will still be based on the pressure drop across the convergent, this will be calibrated against the LDA measurements; furthermore, it will still be possible to perform direct measurements with the LDA, therefore allowing to use the whole range of wind tunnel capabilities.
As can be seen in Fig. 2, the renewed test rig is presently able to reach a maximum airspeed of almost 35 m/s, thereby increasing the high end of the measurement capabilities of the standard. It must also be stressed that the fan engine rotation speed can still be increased by a further 20%, which indicates a potential maximum speed of approximately 40 m/s. This reduction is a precautionary electronic limitation on the engine RPM which will be progressively cut as tests on the facility progress.
This result is interesting as it will allow to perform high-speed calibrations on small anemometers.

4.2 Turbulence profiles:

The turbulence (T_u) level at the various positions was computed as the ratio of the RMS fluctuation of the airspeed measured by the Hot Wire probe to the airspeed itself.
Fig. 5 reports the overall picture obtained by plotting the values thus obtained; different symbols indicate different positions along the wind tunnel axis.
The first observation that can be made is about the absolute level of turbulence. This value is of the order of 0.6 % or less (reaching down to approximately 0.4 % at the lowest speed in position X_1). Such values are of the same order of magnitude as the ones measured before the renovation works, in some positions slightly lower, and in any case never larger. This result is considered as appropriate, as the aim of the present work was not strictly to reduce the turbulence level (which already was good), but to avoid spurious disturbances.
Going now to more specific comments, it can be noticed that values are not strongly influenced by the velocity, although a slight increase can be observed especially for the first position. One notable exception to this statement is the behaviour in the V = 12.5 m/s region, where the T_u level reaches to relatively high values for the most downstream positions (see later).

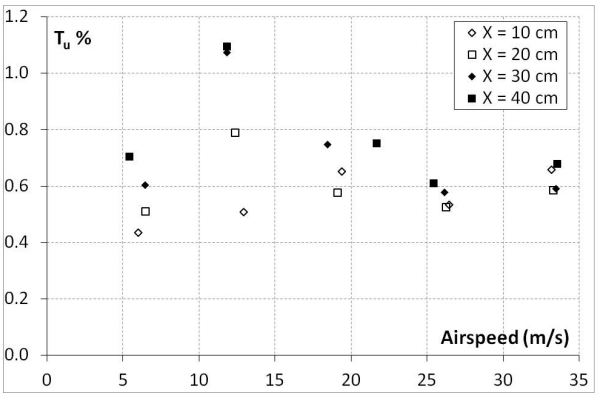

Fig. 5. Turbulence intensities along the test chambers axis as a function of airspeed.

On the other hand, it can also be observed that there is a clear influence of the longitudinal position on the turbulence level at the lower speeds, while this effect is negligible at the higher air velocities.
In order to explain these results, one must recall the structure of the flow in an open-chamber wind tunnel. Actually, at the convergent exit, the flow forms a free shear layer detaching from the nozzle lip as a sequence of ring vortices which subsequently move downstream along the jet. Such vortices can influence the air velocity even into the jet core via potential induction phenomena (see, e.g., [6]). It is therefore believed that the disturbances observed on the axis are connected to the vortical structures.
The position influence on the turbulence level at low speeds is explained by considering that the vortices in this case are larger and maintain their identity for a longer distance, therefore their influence on the centreline will be more important downstream.
The T_u level peak around V = 12.5 m/s, on the other hand, is presumably related to a specific vortex shedding frequency, especially when noticing that the peak grows stronger with X position. It can be speculated that this velocity corresponds to the one when the vortices start to decay before the end of the test chamber; the relatively high turbulence would then be the trace on the axis of the vorticesô collapse.

4.3 Spectral Analysis:

In order to better understand this behaviour and to verify the behaviour of the flow in the test chamber, the velocity signals at the various position were also analysed through Fourier decomposition methods, as described in 3.
Fig. 6 displays the energy density spectra computed at the first measurement position, while Fig. 7 is a plot of the same quantity at the last measurement position; both figures include all the test velocities, reported as the fan RPM. The values are not exactly the same because of the inverter control. Data are plotted limited to a frequency of 100 Hz because the analysis of all frequencies showed no peculiar features beyond this value.

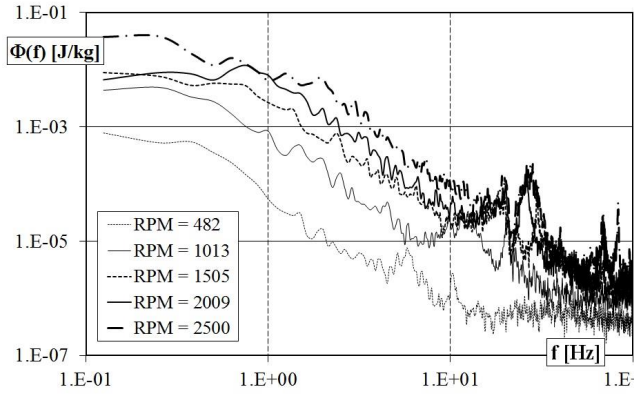

Fig. 6. Energy density spectra at position X_1.

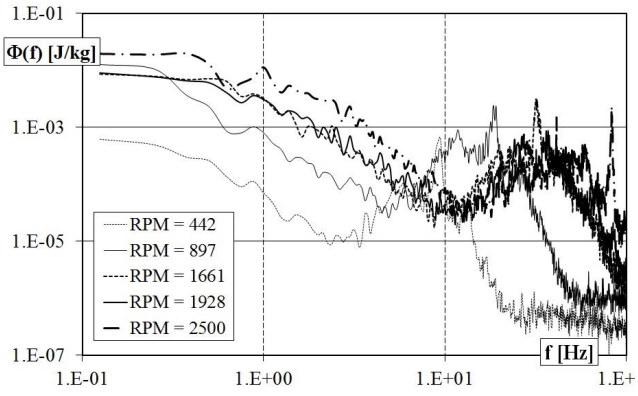

Fig. 7. Energy density spectra at position X_4.

It can be observed that in the first case the spectrum at the lowest speed has a regular behavior, while the one corresponding to the second airspeed value displays an evident peak at a frequency of about 10 Hz. The other three spectra, on the other hand, show much broader peaks at higher frequencies.

Spectra in Fig. 7 display a similar behavior, except that the first spectrum also has a peak at a lower frequency.

First of all, it is important to observe that these plots feature an important difference with respect to their counterparts measured before the works. Specifically, the spectral peaks show up at frequencies depending on the velocities, indicating a real fluid dynamical behavior; in the previous situation, on the contrary, the same frequency showed up at all velocities. This result had been interpreted as the outcome of a mechanical instability, and the present results appear not only to confirm this explanation, but also to show that the mechanical vibration has been eliminated in the new configuration.

The presence of the peaks supports the hypothesis that the turbulence intensity peak at about 12.5 m/s must be related to a phenomenon generated by a high vortex intensity. The reduction of the turbulence at higher speeds is assumed to be the consequence of an earlier vortex decay. Finally, the higher peak at the lower velocity at X_4 is believed to indicate the full development of the shear layer vortices at that position.

5- Conclusions

The first tests on the renewed wind tunnel ñGVPò, which is part of the Italian standard of airspeed, were presented.

The results of such tests are considered to be satisfactory, as they show that the upgrade works met all the objectives. The wind tunnel maximum speed was strongly increased, while reducing the level of vibration and noise.

The turbulence intensity was slightly reduced, providing therefore a better flow quality.

In the near future, this configuration will undergo further tests, specifically a full mapping of the test chamber, a study of the effect of the divergent configuration on the flow regularity and further analysis of the spectral energy density in the test chamber, aimed at better understanding the test rig features.

Acknowledgment

The Authors wish to thank Mr. F. Alasia for his precious help in the definition and design of several mechanical details. The company charged of building the test rig parts (Stillio s.r.l) provided excellent craftsmanship.

The work described in the present paper was funded by INRIM.

References

[1] Piccato A., Spazzini P.G., Malvano R.: *Redesign and Improvement of an Open Circuit Wind Tunnel*, proposed for publication to the journal ñMeccanicaò.

[2] Piccato A., Spazzini P.G., Malvano R.: *Mapping of Flow Features in a wind tunnel*, Proceedings of the 7th International Symposium on Fluid Flow Measurement, Anchorage, Alaska, 2009.

[3] Ferrari, C. *Rendiconti Sperimentali del Laboratorio di Aeronautica del R. Istituto Superiore di Ingegneria di Torinoï 1a Serie ï Determinazione della Caratteristiche della Galleria del Vento.* LôAerotecnica ï V. XIV ï N. 4 ï April 1934.

[4] Bruun, H.H. *Hot-Wire Anemometry*, Oxford University Press, New York, 1985.

[5] Bendat, J.S. and Piersol, A.G. *Random Data: Analysis and Measurement Procedures*, John Wiley and Sons, Inc., New York, 1971.

[6] Todde, V., Spazzini, P.G. and Sandberg, M. *Experimental Analysis of Low-Reynolds Number Free Jets*, Experiments in Fluids, 2009.